Chemistry & Biology
Article

# Design and Characterization of a Broad -Spectrum Bactericidal Acyl-lysyl Oligomer

Liran Livne,[1] Tchelet Kovachi,[1] Hadar Sarig,[1] Raquel F. Epand,[2] Fadia Zaknoon,[1] Richard M. Epand,[2] and Amram Mor[1,*]
[1]Department of Biotechnology and Food Engineering, Technion-Israel Institute of Technology, Haifa 32000, Israel
[2]Department of Biochemistry and Biomedical Sciences, McMaster University, Hamilton, Ontario, L8N 3Z5, Canada
*Correspondence: amor@tx.technion.ac.il
DOI 10.1016/j.chembiol.2009.11.012

## SUMMARY

**Previously characterized chemical mimics of host defense peptides belonging to the oligo-acyl-lysyl (OAK) family have so far failed to demonstrate broad-spectrum antibacterial potency combined with selectivity toward host cells. Here, we investigated OAK sequences and characterized a promising representative, designated $C_{12}K$-3$\beta_{10}$, with broad-spectrum activity ($MIC_{90}$ = 6.2 μM) and low hemotoxicity ($LC_{50}$ > 100 μM). Whereas $C_{12}K$-3$\beta_{10}$ exerted an essentially bactericidal effect, *E. coli* bacteria were killed faster than *S. aureus* (minutes versus hours). Mechanistic studies addressing this difference revealed that unlike *E. coli*, *S. aureus* bacteria undergo a transient rapid bactericidal stage that over time converts to a bacteriostatic effect. This behavior was dictated by interactions with cell wall-specific components. Preliminary efficacy studies in mice using the thigh infection model demonstrated the OAK's ability to significantly affect bacterial viability upon single-dose systemic treatment (2 mg/kg).**

## INTRODUCTION

Mounting efforts are underway to identify and develop novel therapies to help deal with current and emerging resistant pathogens (Cassell, 1997; Parisien et al., 2008). Host defense peptides (HDPs), part of the innate immune system, represent attractive candidates for clinical development due to their ability to target a broad spectrum of pathogens while significantly challenging development of resistance mechanisms (Bradshaw, 2003; Hancock and Sahl, 2006). Although various details of the mechanism of action are not fully understood, it is now widely believed that HDPs can affect bacterial viability through a multitude of non-receptor-meditated interactions (Brogden, 2005; Zasloff, 2002) including interference with cell wall (Epand et al., 2008a; Harder et al., 2001) and cell membrane (Heller et al., 1998; Shai, 2002; Wu et al., 1999) integrity, as well as inhibition of essential intracellular processes (Boman et al., 1993; Couto et al., 1993; Cudic and Otvos, 2002; Patrzykat et al., 2002).

As drug candidates, however, HDPs present various drawbacks including toxicity and bioavailability as well as production costs issues (Bradshaw, 2003; Gordon et al., 2005). To overcome these disadvantages, peptide-mimetic compounds have been designed based on essential biophysical characteristics of HDPs: charge, hydrophobicity, and amphipathic organization (Rotem and Mor, 2009). The most studied examples of such mimics are represented by (1) β peptides (Liu and DeGrado, 2001; Porter et al., 2005), a class of polyamides composed of β amino acids; (2) peptoids (Kirshenbaum et al., 1998; Patch and Barron, 2003), stable secondary structure oligomers of N-substituted glycines; (3) arylamide oligomers (Tew et al., 2002); and (4) oligomers of acylated lysines (OAKs) (Radzishevsky et al., 2007a, 2007b). At least one version of each of these classes of mimics was reported to combine potent antibacterial activity with low hemolytic activity. However, while β peptides and peptoids are considered relatively difficult and expensive to synthesize (Tew et al., 2002), the most recent arylamide derivatives (based on phenylene ethynylene oligomers) and OAKs seem of particular structural simplicity whose preliminary assessment shows significant promise as potential candidates for systemic therapy (Choi et al., 2009; Sarig et al., 2008).

The basic OAK molecular organization consists of tandem repeats of acyl-lysyl or lysyl-acyl-lysyl subunits, termed $\alpha_i$ and $\beta_i$, respectively, where i specifies the acyl length. The acyl chains of OAKs reported so far contained either 4, 8, or 12 carbon atoms (Radzishevsky et al., 2008). Their analysis revealed that selective OAKs were all based on butyroyl and (mostly) octanoyl moieties and targeted essentially Gram-negative bacteria, whereas the lauroyl-based OAKs generally displayed poor and non-selective antibacterial properties clearly associated with high tendency for self-assembly in aqueous media (Radzishevsky et al., 2008; Sarig et al., 2008). More recently, non-hemolytic sequences, such as $NC_{12}$-2$\beta_{12}$ (Zaknoon et al., 2009) and $C_{12(\omega 7)}K$-$\beta_{12}$ (Epand et al., 2009), were reported, but these short OAKs targeted essentially Gram-positive species only. Overall, these studies have indicated that while selective antimicrobial activity emerged gradually upon increasing hydrophobicity (e.g., from C4 to C8 acyls) it was reduced in longer acyls due to excess hydrophobicity, thereby suggesting that OAKs with intermediate acyls might be more suitable for improved properties. Here, we report the design and the antibacterial properties of a series of new decanoyl-based derivatives as well as the characterization of the most promising representative.

## RESULTS

### Structure-Activity Relationship Studies

Table 1 summarizes the biophysical properties of three series of new OAKs, all starting with the N terminus, lauroyl-lysyl ($C_{12}K$), and including up to five α or β subunits. Figure 1 summarizes

**Table 1. Biophysical Properties of α- and β-OAKs**

| OAK | MW | Q[a] | H[b] (%) | $LC_{50}$[c] (μM) | CAC[d] (μM) |
|---|---|---|---|---|---|
| $\alpha_{10}$ series | | | | | |
| $C_{12}K\text{-}1\alpha_{10}$ | 624.6 | 2 | 53.5 | 55.6 | 42 |
| $C_{12}K\text{-}2\alpha_{10}$ | 922 | 3 | 52.4 | 29.4 | 40 |
| $C_{12}K\text{-}3\alpha_{10}$ | 1219.5 | 4 | 51.6 | 10.0 | 40 |
| $C_{12}K\text{-}4\alpha_{10}$ | 1517 | 5 | 51.3 | 4.5 | 20 |
| $C_{12}K\text{-}5\alpha_{10}$ | 1814.4 | 6 | 50.2 | <3.1 | 10 |
| $\beta_{10}$ series | | | | | |
| $C_{12}K\text{-}1\beta_{10}$ | 752.8 | 3 | 49.0 | >100 | >100 |
| $C_{12}K\text{-}2\beta_{10}$ | 1178.4 | 5 | 45.9 | >100 | >100 |
| $C_{12}K\text{-}3\beta_{10}$ | 1604 | 7 | 44.9 | >100 | >100 |
| $C_{12}K\text{-}4\beta_{10}$ | 2029.7 | 9 | 44.7 | >100 | >100 |
| **$\beta_8$ series** | | | | | |
| $C_{12}K\text{-}1\beta_8$ | 724.8 | 3 | 47.0 | >100 | >100 |
| $C_{12}K\text{-}2\beta_8$ | 1122.3 | 5 | 44.9 | >100 | >100 |
| $C_{12}K\text{-}3\beta_8$ | 1519.9 | 7 | 43.8 | >100 | >100 |
| $C_{12}K\text{-}4\beta_8$ | 1917.4 | 9 | 43.2 | >100 | >100 |

[a] Total charge.
[b] Molecular hydrophobicity estimated by elution time in reverse-phase HPLC.
[c] Lytic concentration is the OAK concentration that caused 50% hemolysis after 3 hr incubation with 1% red blood cells in PBS, estimated from a dose-dependent study.
[d] Critical aggregation concentration, estimated from a concentration-dependent study of light scattering in PBS.

their antibacterial potency in terms of the minimal inhibitory concentration (MIC) assessed against two test bacteria, *Escherichia coli* and *Staphylococcus aureus*, respectively representing Gram-negative and Gram-positive bacteria. For purposes of comparison, Figure 1 also includes MIC values of previously reported OAK analogs (i.e., octanoyl- and dodecanoyl-based α-OAKs and dodecanoyl-based β-OAKs) (Radzishevsky et al., 2008). The structure-activity relationship that emerged from this study indicated that the more hydrophobic $\alpha_{10}$-OAKs generally behaved similarly to their $\alpha_{12}$ counterparts (Radzishevsky et al., 2008) in that they displayed a tendency for hemolysis and for self-assembly; both properties increased with an increasing number of subunits (Table 1) and, albeit comparatively, antibacterial activity was somewhat improved (Figure 1). In contrast, the slightly less hydrophobic $\beta_{10}$-OAKs series exhibited significantly reduced hemolytic and self-assembly properties, while a few displayed potent antibacterial activity, such as $C_{12}K\text{-}3\beta_{10}$ (MIC values are 3.1 and 6.2 μM). The fact that the corresponding $\beta_8$-OAKs were generally less active was clearly associated with lack of optimal charge (Q) or hydrophobicity (H): compare, for instance, $C_{12}K\text{-}3\beta_{10}$ with $C_{12}K\text{-}2\beta_8$ (having identical H) and with $C_{12}K\text{-}3\beta_8$ (having identical Q). Note that the effect of culture media on OAKs aggregation properties is negligible, as was recently reported for a more hydrophobic analog, $NC_{12}K\text{-}3\beta_{12}$ (Held-Kuznetsov et al., 2009).

## Characterization of the Antimicrobial Activity of $C_{12}K\text{-}3\beta_{10}$

Data presented in Table 2 confirmed that $C_{12}K\text{-}3\beta_{10}$ is endowed with broad spectrum antibacterial activity. MIC experiments

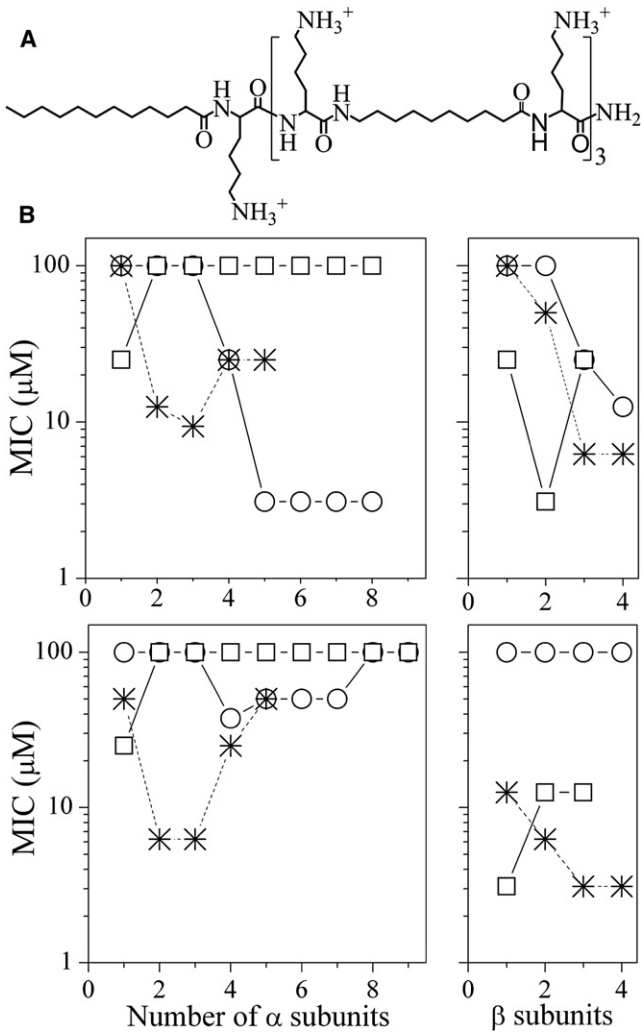


**Figure 1. Structure of $C_{12}K\text{-}3\beta_{10}$ and Its Structure-Activity Relationships**

(A) Molecular structure of $C_{12}K\text{-}3\beta_{10}$.

(B) Effects of the number of α and β subunits (left and right, respectively) on the MIC value of OAKs sharing a common N terminus (dodecanoyl-lysyl) and varying in sequence. Subunits composed of octanoyl, decanoyl, and dodecanoyl are represented with circles, asterisks, and rectangles, respectively. MICs were determined after overnight incubation of each OAK with 2–4 × $10^5$ cfu/ml with *E. coli* ATCC 35218 (top) and *S. aureus* ATCC 29213 (bottom) in LB medium.

performed against clinically relevant representatives of both Gram-positive and Gram-negative species revealed that while the OAK exerted an average 2-fold higher potency over the Gram-positive species, 92% of the 49 bacterial strains tested were fully inhibited at 1.6–6.2 μM, including multidrug-resistant strains.

## Mechanistic Studies

### *Bactericidal Kinetics*

Given the inherent differences in MIC values between Gram-positive and Gram-negative bacteria, the mode of action of $C_{12}K\text{-}3\beta_{10}$ was investigated against two different strains of

**Table 2. Antibacterial Activity of $C_{12}K\text{-}3\beta_{10}$ Against a Panel of Bacteria**

| Bacteria (Number of Strains Tested) | MIC Range (μM) |
|---|---|
| Gram-negative species | |
| *Escherichia coli* (n = 13) | 3.1–6.2 |
| *Pseudomonas aeruginosa* (n = 11) | 3.1–6.2 |
| *Acinetobacter spp.* (n = 3) | 1.6–12.5 |
| *Salmonella spp.* (n = 2) | 6.2 |
| Gram-positive species | |
| *Staphylococcus spp.* (n = 9) | 1.6–12.5 |
| *Listeria spp.* (n = 5) | 1.6–3.1 |
| *Bacillus spp.* (n = 3) | 6.2–25 |
| *Streptococcus spp.* (n = 2) | 1.6 |
| *Enterococcus faecalis* (n = 1) | 6.2 |

both *E. coli* bacteria (MICs were 3.1 and 6.2 μM) and *S. aureus* bacteria (MICs were 3.1 and 6.2 μM) using three different concentrations corresponding to one, three, and six multiples of the respective MIC values. Figure 2A summarizes a representative outcome for *E. coli* (MIC 3.1 μM) and *S. aureus* (MIC 6.2 μM). As shown in Figures 2A1 and 2A2, the OAK significantly reduced the colony-forming unit (cfu) count in a time- and dose-dependent manner, indicating that $C_{12}K\text{-}3\beta_{10}$ exerted an essentially bactericidal effect against both bacterial species. However, the time-kill curves against *E. coli* were swifter, achieving near complete elimination of bacteria within 3 hr or less, for all tested concentrations. In contrast, when encountering *S. aureus*, $C_{12}K\text{-}3\beta_{10}$ displayed slower kinetics of killing, which over time reached a bacteriostatic stage. Similar results were obtained using additional strains of each bacteria but with inversed MIC potencies (data not shown), suggesting that the differential killing rates reflect genuinely different mechanisms of action.

### *Damaged Cytoplasmic Membrane*

Extracellular ATP was measured under the time-kill conditions as compared with the dermaseptin derivative S4(1–16), known for its powerful membrane-disruptive properties (Rotem et al., 2008). Figures 2B1 and 2B2 show that when added to *E. coli* cultures, $C_{12}K\text{-}3\beta_{10}$ induced an intensive, dose-dependent leakage of ATP as indicated by the increase in luminescence, unlike in *S. aureus*, where a partial ATP leakage could be observed at all tested concentrations but only at the initial stage of the interaction.

### *Depolarization Studies*

Our attempts to verify whether the OAK induced plasma membrane depolarization [as observed with previously described OAKs (Rotem et al., 2008)] revealed that $C_{12}K\text{-}3\beta_{10}$ caused a nearly immediate depolarization of both *E. coli* and *S. aureus* plasma membranes (Figures 2C1 and 2C2). However, unlike *E. coli*, depolarization of *S. aureus* was partial, as indicated by the positive control. The OAK's ability to rapidly disrupt the cytoplasmic membrane of *E. coli* was also confirmed by its ability to induce rapid cleavage of the chromogenic substrate ONPG by the intracellular enzyme β-galactosidase using the *E. coli* mutant ML-35 (data not shown). Interestingly, permeabilization studies with model membranes mimicking the composition of Gram-positive or Gram-negative bacteria did not allow release of molecules ~400 Da from internal contents of large unilamellar vesicles (data not shown), up to 40 μM OAK. This result underlines the importance of testing membrane permeabilization with the bacteria themselves.

Thus, different experimental approaches converged to support the view that $C_{12}K\text{-}3\beta_{10}$ exerted bactericidal activities but the OAK seems to achieve this effect by the rapid disruption of the plasma membrane. Over time, however, membrane disruption is inhibited in *S. aureus*, although not the OAK's ability to affect bacterial proliferation, as shown by the MIC experiments. To shed light into the possible reason(s) for these observations, we next assessed the OAK's binding properties to well known targets of OAKs and HDPs: cell wall components [lipopolysaccharide (LPS) and lipoteichoic acid (LTA) (Epand et al., 2008a; Falla et al., 1996; Majerle et al., 2003)], model phospholipid membranes with compositions known to mimic the plasma membranes (Epand et al., 2008b; Gaidukov et al., 2003; Rotem et al., 2008), and plasmidial DNA representing an intracellular bacterial target (Rotem et al., 2008).

## Binding Properties

### *Binding to Cell Wall Components by Isothermal Titration Calorimetry (ITC)*

Binding of $C_{12}K\text{-}3\beta_{10}$ to LPS of *E. coli* O111:B4 was found to be endothermic. The heats of reaction obtained by ITC are the result of several interactions that play a part in the binding process of OAKs, presenting a balance of hydrophobic and electrostatic moieties with such complex macromolecules as LPS, where hydrogen bonding rearrangements, aggregation phenomena, and cation replacement can take place. Nevertheless, it is clear from Figure 3A that a rapid decrease in ΔH at low molar concentrations of OAK (comparable to the MIC), resulting from the integration of each of the peaks obtained experimentally, is due to rapid binding of the cationic OAK with the negatively charged phosphate groups of the LPS. A similar result was obtained with LPS from the *P. mirabilis* polymyxin-resistant strain R45 when titrated with polymyxin B (Howe et al., 2007), where the entropically determined free energy is the result of the endothermic enthalpy change exceeding the exothermic enthalpy change of the electrostatic attraction. The ITC titration of the cationic antimicrobial peptides temporins A, B, or L with LPS from *E. coli* O26:B6 was also found to be endothermic (Mangoni et al., 2008). The course of the titration in LPS explains the rapid access of OAK to the Gram-negative bacterial cytoplasmic membrane, in accordance to the idea of self-promoted uptake (Hancock, 1997; Piers et al., 1994).

A different picture emerges from the titration of LTA from *S. aureus*. At concentrations comparable to the MIC, the OAK initially neutralizes negative charge in LTA in an enthalpically driven reaction, but charge attraction is quickly overcome by endothermic forces, and over a large range of subsequent OAK additions very little change is observed (Figure 3B). We highlight the initial steps in the reaction with LTA by repeating the titration with only six additions of 1.4 μM OAK each to LTA in the cell (Figure 3C). In comparison with the titration into LPS, the changes in enthalpy seen with LTA are rather modest. Reorganization of the hydrogen bonding network in LTA (which is part

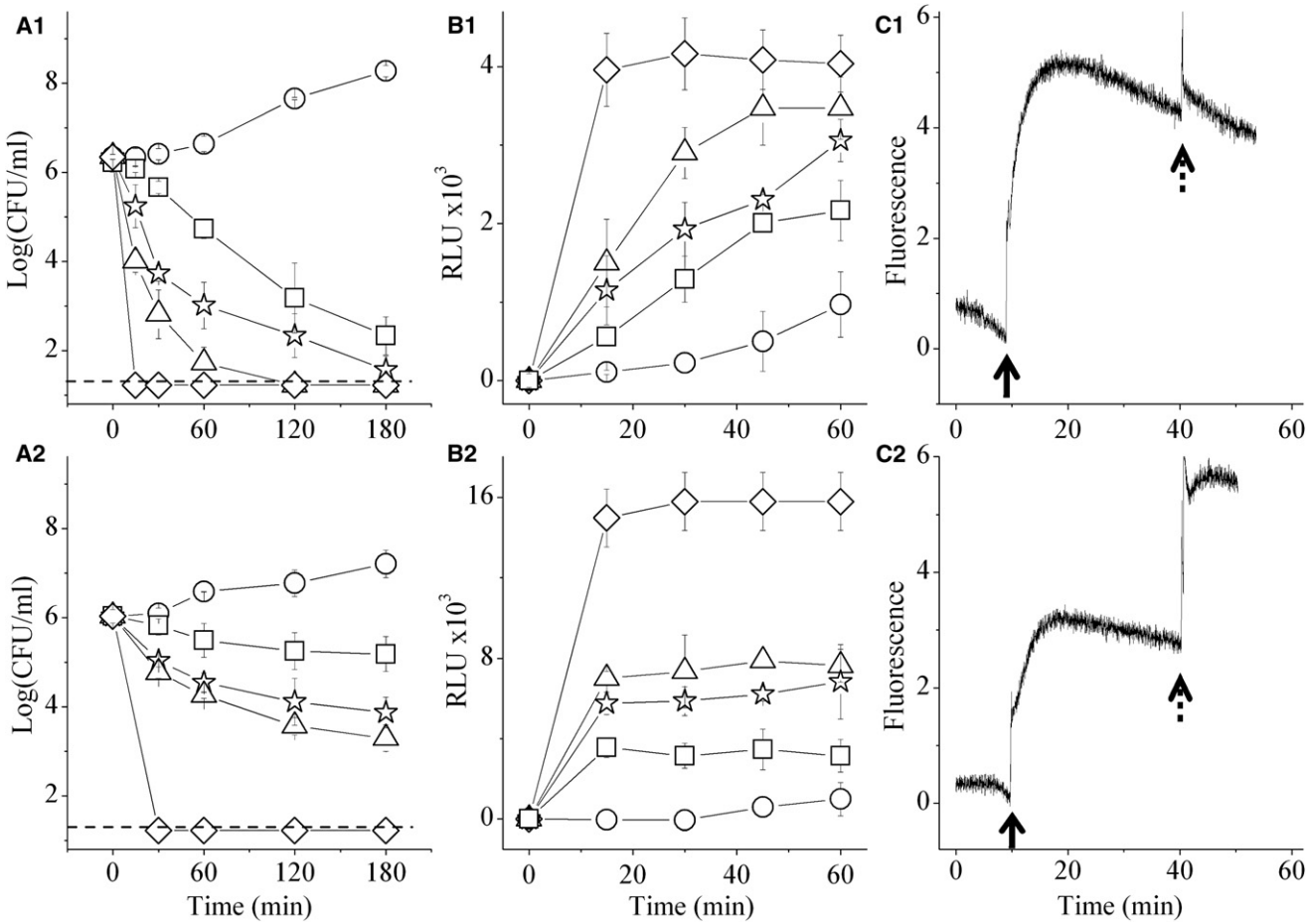


**Figure 2. Mechanistic Studies**

The mechanism of action was investigated against both *E. coli* 35218 (top) and *S. aureus* 29213 (bottom).

(A1 and A2) Bactericidal kinetics (MIC values were 6.2 and 3.1, respectively). Diamonds, positive control, dermaseptin S4(1–16) at 6× MIC; circles, untreated control; squares, stars, and triangles, $C_{12}$K-3$\beta_{10}$ at 1×, 3×, and 6× MIC, respectively. Error bars represent ± SD.

(B1 and B2) Extracellular ATP levels in treated bacterial suspensions. Symbols and concentrations are as in (A). Error bars represent ± SD.

(C1 and C2) Representative experiments for cytoplasmic-membrane depolarization. The baseline drift is due to a worn out instrument lamp. Solid and dotted arrows refer respectively to time for addition of $C_{12}$K-3$\beta_{10}$ (t = 10 min) and dermaseptin S4(1–16) (t = 40 min) at 6× MIC each.

of the thick peptidoglycan layer of Gram-positive bacteria), coupled with hydrophobically driven interactions with the OAK's acyl chains, counteract the effect of the seven positive charges in $C_{12}$K-3$\beta_{10}$. The difference between this titration with LTA of *S. aureus* and a similar study using the OAK $C_{12(w7)}$K-$\beta_{12}$, which resulted in an exothermic process driven by electrostatic forces (Epand et al., 2009), lies in the size and number of charges in the two different OAKs. The $C_{12(w7)}$K-$\beta_{12}$ has three cationic groups that permit electrostatic interaction with LTA, but its smaller size and the presence of a double bond in the N-terminal acyl chain allow it a more facile entry into the peptidoglycan layer. The sequence $C_{12}$K-3$\beta_{10}$ has seven charges evenly distributed in a larger molecule with hydrocarbon chains separating them, resulting in a tighter association. The course of the titration with LTA is in accord with the initial bactericidal effect of the OAK in Gram-positive bacteria, which is followed quickly by a truncated depolarization, loss of ATP, and reversal to a bacteriostatic regime.

### *Binding to Phospholipid Model Membranes by Surface Plasmon Resonance*

We studied mimics of the cytoplasmic membrane of *S. aureus* and *E. coli*: phosphatidylglycerol (PG):cardiolipin (CL) and PG:phosphatidylethanolamine (PE), respectively (Epand et al., 2008b; Lohner and Prenner, 1999). Figure 4A depicts typical dose-dependent association/dissociation curves used to derive the binding constants, using the two-step binding model (Gaidukov et al., 2003). The data indicated that the OAK has high affinity for both types of membranes as shown in the adhesion step ($K_{adhesion}$ 3.2 × $10^5$ and 1.4 × $10^5$ $M^{-1}$, respectively). These values are comparable to those obtained with other active OAKs (Rotem et al., 2008) and HDPs (Gaidukov et al., 2003). Thus, although the apparent affinity constants ($K_{app}$) for PG:CL and PG:PE were rather similar, the data indicate that the OAK has higher tendency for adhering to the highly anionic membrane mimic of *S. aureus* compared with that of *E. coli* (approximately 2-fold) but has even higher tendency for insertion (approximately

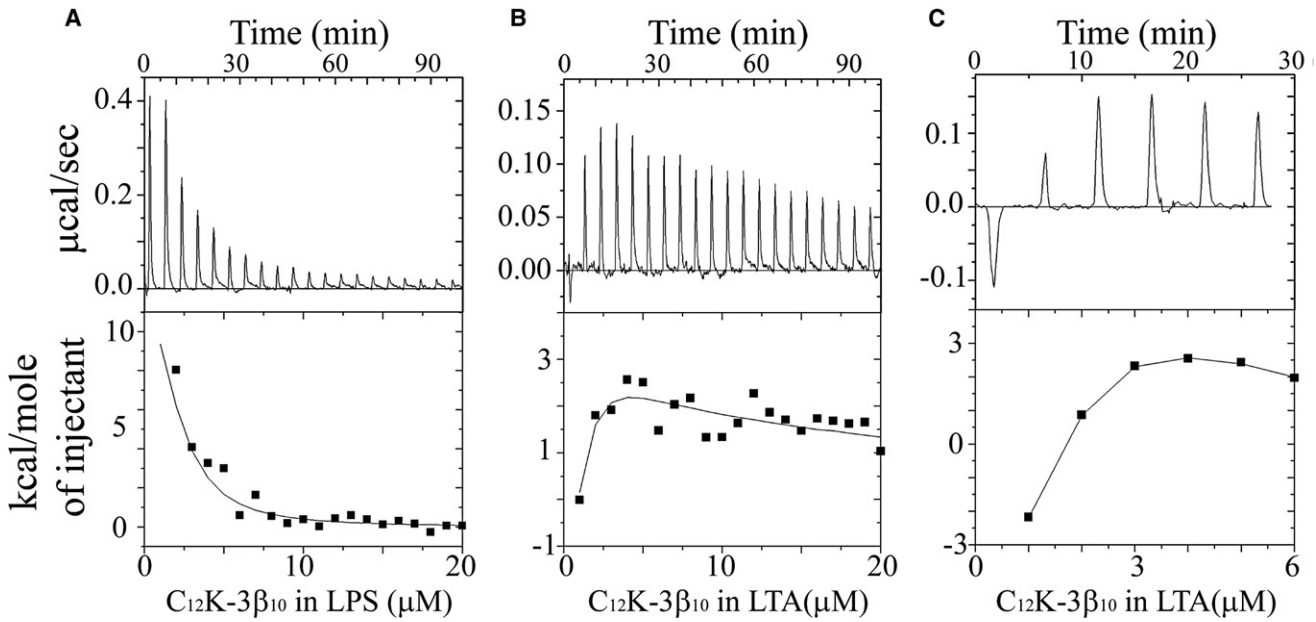


**Figure 3. OAK Interaction with Cell-Wall Components**

Shown are ITC curves obtained by titrating 10 µl of 0.2 mM OAK in the syringe into 125 µg/ml LPS (A) or LTA (B and C) in the cell, at 30°C. Buffer was 10 mM HEPES and 140 mM NaCl (pH 7.4). Cell volume was 1.4276 ml. The top panels represent heat flow (µcal/s) as a function of time (min). The points in the bottom panels present the result of integrating each peak in the top panel (kcal/mole of OAK) as a function of OAK concentration in the cell (µM).

3-fold) into the latter, which correlated well with the kinetic rates observed above (Figure 2). In *S. aureus*, as with most Gram-positive bacteria, the main components of the cytoplasmic membrane are lipids with negatively charged headgroups with little or no zwitterionic ones present, although there are some exceptions in the species *Bacillus* or *Clostridium* that contain a certain amount of PE, but with anionic lipids predominating. The binding parameters in both types of model membranes are rather similar. However, the insertion parameters (Figure 4A) clearly indicate that the OAK inserts into PG:PE with about three times more affinity than into PG:CL, thus causing deeper disruption in the headgroup area of the bilayer of membranes containing zwitterionic lipids. This greater perturbation supports the more efficient membrane permeabilization observed in *E. coli*.

Binding constants were also calculated for the interactions with a PC/cholesterol model mimicking the membrane of erythrocyte. $C_{12}$K-3$\beta_{10}$ displayed lower binding affinity for such a membrane, in accordance with the observed low hemolytic activity (Table 1).

### *Binding to Bacterial DNA*

We tested the OAK's ability to protect the purified *E. coli* plasmid pUC19 from digestion by restriction enzymes (ScaI or BamHI). As shown in Figure 4B, unlike the analog $C_{12}$K-7$\alpha_8$, known for its DNA binding properties (Radzishevsky et al., 2007b; Rotem et al., 2008), $C_{12}$K-3$\beta_{10}$ did not prevent plasmid digestion, thereby arguing against the possibility of nucleic acids acting as potential targets of this OAK.

### Efficacy Studies

The ability of $C_{12}$K-3$\beta_{10}$ to systemically affect bacterial viability in vivo was assessed using the thigh infection model where mice were inoculated intramuscularly with *S. aureus* and treated subcutaneously. To determine efficacy, mice were sacrificed, and the thigh muscle was homogenized and plated for cfu enumeration. As shown in Figure 5, by using the systemic route, $C_{12}$K-3$\beta_{10}$ has managed to reduce bacterial count in the infected muscle (96% reduction in cfu count) after administration of a single dose of 2 mg/kg. Thus, $C_{12}$K-3$\beta_{10}$ has significantly ($p < 0.0001$) reduced bacterial load, similarly to the positive control (vancomycin) administered at 20 mg/kg.

## DISCUSSION

The decanoyl-based OAKs presented biophysical properties that stand in line with previous observations (Radzishevsky et al., 2005, 2007a, 2008; Sarig et al., 2008). Namely, two main trends can be identified from the structure-activity relationships study: bactericidal activity deteriorates with increasing tendency for self-assembly, in accordance with the view that self-assembly tends to obstruct activity of OAK sequences that display near-optimal HQ properties and might otherwise be active (Radzishevsky et al., 2008). This can explain, at least partly, why hydrophobic $\alpha_{10}$-OAKs exhibited poor antibacterial activity. The other visible trend pertains to the "bell-shaped" relationships existing between backbone length and antibacterial potency, as depicted in Figure 1. Thus, while the shortest $\alpha_{10}$-OAK was barely active, longer derivatives showed enhanced activities, which deteriorated in the longest sequences. This behavior complies with the occurrence of an optimal HQ window for each OAK series, as previously rationalized (Radzishevsky et al., 2008). In fact, the optimum obtained for $\alpha_{10}$-OAKs fits right between those of $\alpha_8$- and $\alpha_{12}$-OAKs, for both *E. coli* and

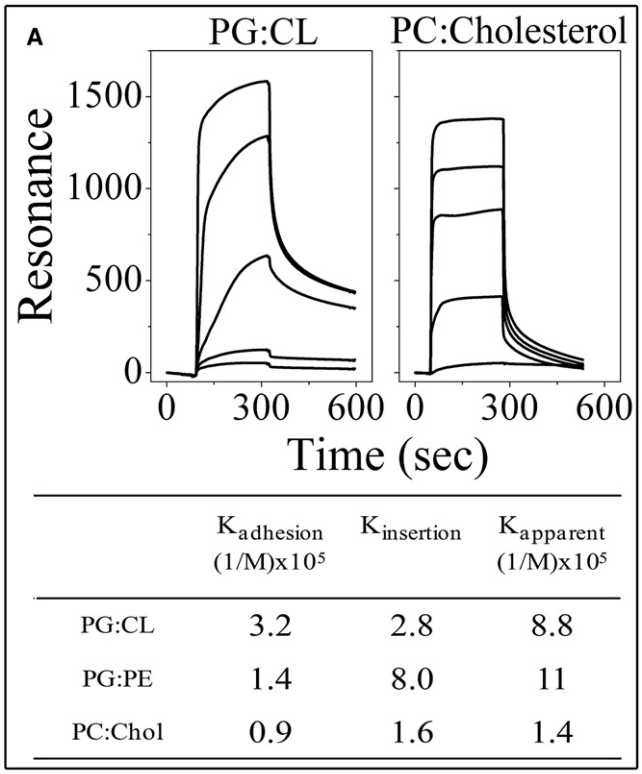


| | $K_{adhesion}$ (1/M)x$10^5$ | $K_{insertion}$ | $K_{apparent}$ (1/M)x$10^5$ |
|---|---|---|---|
| PG:CL | 3.2 | 2.8 | 8.8 |
| PG:PE | 1.4 | 8.0 | 11 |
| PC:Chol | 0.9 | 1.6 | 1.4 |

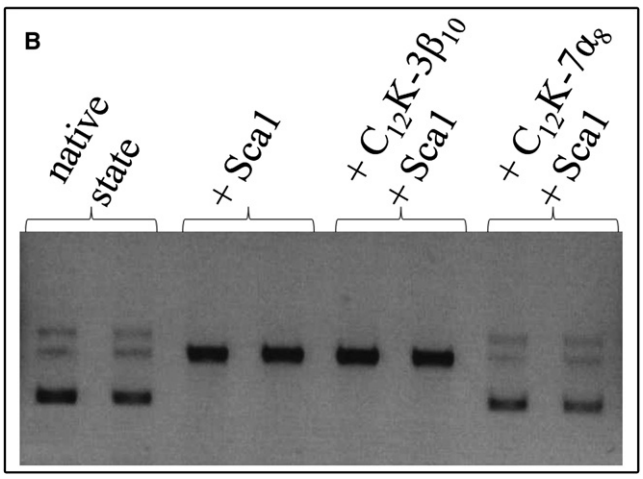


**Figure 4. Binding Properties to Model Bilayer Membranes and DNA**

(A) Top panels depicts representative binding curves (five OAK concentrations) obtained with PG:CL (60:40) and PC:Cholesterol (90:10). Bottom panel summaries the affinity constants as analyzed by local fitting using the two stage binding model.

(B) Duplicated agarose gel runs of the *E. coli* plasmid pUC19 (150 ng) in its native state and after exposure to ScaI. Last four lanes show pUC19 after pre-incubation (prior to exposure to ScaI) with $C_{12}$K-3$\beta_{10}$ (6× MIC) and the OAK analog $C_{12}$K-7$\alpha_8$ (positive control), respectively.

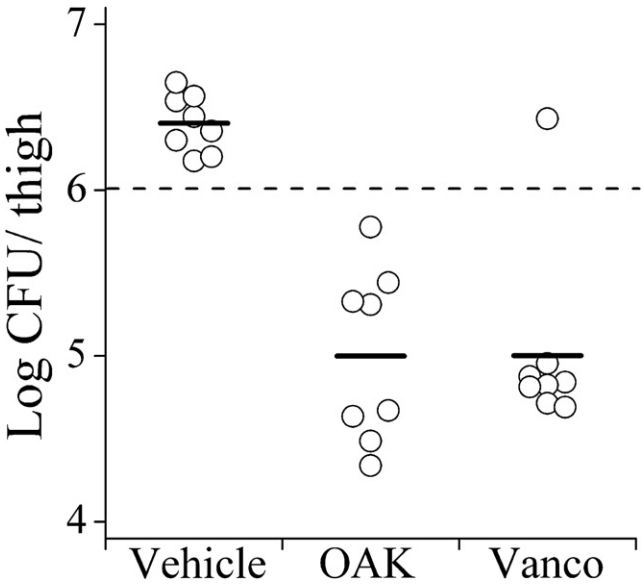


**Figure 5. Ability of $C_{12}$K-3$\beta_{10}$ to Affect Bacterial Viability Systemically Using the Thigh Infection Model**

Mice (n = 8/group) were inoculated intramuscularly with $10^6$ cfu of *S. aureus* (ATCC 29213) and treated 2 hr after inoculation with $C_{12}$K-3$\beta_{10}$ (OAK; 2 mg/kg) or vancomycin (VANCO; 20 mg/kg) as a positive control. Vehicle mice were treated with PBS. Dashed and solid horizontal bars respectively show the mean values for the initial inoculums and post-treatment counts.

*S. aureus*. A similar trend could probably be observed for the $\beta_{10}$-OAKs as well, as seen in the behavior of the $\beta_{12}$ series. One beneficial outcome of this systematic behavior is the possibility to predict improved activities, as shown with $C_{12}$K-3$\beta_{10}$.

Interestingly, while we find that $C_{12}$K-3$\beta_{10}$ exerted an essentially bactericidal activity against both Gram-negative and Gram-positive bacteria, our comparison of functional and mechanistic properties has provided evidence for the coexistence of subtle differences in the modalities by which $C_{12}$K-3$\beta_{10}$ can inflict death upon bacteria, namely when they belong to different bacterial species. This phenomenon was often observed with a variety of HDPs as well, but was not experimentally addressed (Ge et al., 1999; Giangaspero et al., 2001; Pag et al., 2004; Sahl et al., 2005). Our study indicates that the peptide interactions with both the cell wall and plasma membrane can be implicated in determining the final outcome. Based on the presented data we propose the following scenario of events: $C_{12}$K-3$\beta_{10}$ is initially attracted to both types of bacteria, is driven by electrostatic forces, and sequentially undergoes multiple interactions with components of both cell walls (namely LPS and LTA). Subsequently, in Gram-negative species, the OAK manages to rapidly reach the plasma membrane, much as described by the self-promoted uptake theory (Falla et al., 1996; Hancock, 1997; Piers et al., 1994), and interferes with its barrier function as a result of the compelling tendency for insertion (Figure 4A). This typically results in rapid membrane depolarization (Figure 2C), hence the observed leakage of solutes (Figure 2B).

In contrast, in Gram-positive bacteria, the OAK can undergo a dual time-dependent fate. The first OAK molecules manage to easily reach and disrupt the cytoplasmic membrane, similarly to Gram-negative bacteria, hence the initial rapid (but partial) membrane disruption observed in both the ATP leakage and depolarization assays (Figure 2). However, on the way toward the plasma membrane, part of the incoming OAK molecules associate tightly with the peptidoglycan layer. In time, OAK accumulation may block/impair access of substrates in and

out of the cell, including access of additional OAK molecules, to the plasma membrane, roughly as previously proposed for another non-peptide HDP mimic (Epand et al., 2008a). Such a blockage can shift the OAK mode of action from bactericidal to bacteriostatic in a time-dependent manner, as observed in the flat *S. aureus* time-kill curves or ATP leakage kinetics. These mechanisms are supported by data in Figures 3B and 3C.

Various β-OAKs were previously shown to resist plasma proteases and other plasma components (Held-Kuznetsov et al., 2009; Radzishevsky et al., 2008), thus predicting that β-OAKs could maintain bioavailability and antibacterial activity in vivo. Here, we presented evidence showing that $C_{12}$K-3$\beta_{10}$ was efficient in reducing viability of bacteria such as *Staphylococcus aureus*, an important pathogen that is responsible for a variety of diseases (Zetola et al., 2005). Thus, unlike previously published OAKs, shown to be active in vivo using the peritonitis-sepsis model (a model in which both bacteria and treatment are administrated within the same area), our current findings (Figure 5) suggest the potential of $C_{12}$K-3$\beta_{10}$ to be useful as a systemic antibacterial compound.

## SIGNIFICANCE

**Previous OAK series have established the importance of HQ properties in generating a non-hemolytic antibacterial compound. Although several OAK sequences indeed displayed improved properties, they failed so far to demonstrate a combination of broad-spectrum antibacterial potency as well as selectivity relative to host cells. The present study has illustrated the predictive potential of this simple HDP mimetic system toward achieving improved properties. Thus, this study unraveled the first non-hemolytic broad-spectrum antibacterial OAK and, furthermore, provided mechanistic evidence that might explain similar kinetic differences observed with HDPs. By virtue of its antibacterial potency and low hemocytotoxicity, the OAK described in this study represents a potential candidate for a variety of antibacterial applications, including for therapeutic development.**

## EXPERIMENTAL PROCEDURES

### Synthesis

The OAKs were synthesized by the solid-phase method applying the *N*-(9-fluorenyl)methoxycarbonyl (Fmoc) active ester chemistry (Fields and Noble, 1990) essentially as described (Radzishevsky et al., 2008), using Fmoc-10-Aminodecanic acid and Fmoc-Lysine. 4-methylbenzhydrylamine resin was used to obtain amidated OAKs. The crude OAKs were purified to chromatographic homogeneity (>95% purity) by reverse-phase high-pressure liquid chromatography (HPLC) and subjected to mass spectrometer analysis (Alliance-ZQ; Waters). HPLC runs were performed on preparative and then on analytical $C_{18}$ columns (Vydac) using a linear gradient of acetonitrile in water (1%/minute), with both solvents containing 0.1% TFA. Purified OAKs were stocked as lyophilized powder at −20°C. Prior to being tested, fresh solutions were prepared in water (mQ; Millipore), vortexed, sonicated, centrifuged, and then diluted in the appropriate medium.

### Organization in Solution

The OAKs' self-assembly properties were investigated by static light scattering measurements on a Jobin-Yvon Horiba Fluorolog-3 with FluorEssence (Tanford, 1980) as described previously (Radzishevsky et al., 2008). Briefly, serial 2-fold dilutions of the OAKs were prepared in phosphate-buffered saline (PBS) and incubated for 2 hr at room temperature, and the light scattering of each dilution was measured by holding both the excitation and the emission at 400 nm (slit width, 1 nm). To describe the dependence of the scattered signal on the OAK concentration, the intensity of scattered light was plotted against the total OAK concentrations. Since the light-scattering signal is proportional to the number of aggregated molecules and the size of the aggregate, the slope is indicative of the aggregation tendency and reveals the aggregation properties, and a slope value above unity indicates the presence of an aggregative form.

### Hemolytic Activity

The OAKs' capacity to induce hemoglobin leakage was determined against human red blood cells after 3 hr of incubation in PBS [50 mM sodium phosphate and 150 mM NaCl (pH 7.4)] at 37°C in the presence of a hematocrit of 1%, as described previously (Radzishevsky et al., 2008).

### Antibacterial Assays

Bacteria tested were *Escherichia coli* (ATCC 35218, ATCC 25922, ML35, and ten clinical isolates), *Pseudomonas aeruginosa* (ATCC 9027, ATCC 27853, and nine clinical isolates), *Staphylococcus aureus* (ATCC 29213, ATCC 25923, ATCC 43300, and five clinical isolates), *Enterococus faecalis* (ATCC 29212), *Streptococcus agalactiea* (ATCC 13813), *Streptococcus pneumoniae* (ATCC 6303), *Bacillus cereus* (ATCC 11778), *Bacillus subtilis (*BR151), *Bacillus polymyxa* (ATCC 842), *Listeria welshineri* (ATCC 35897), *Listeria innocua* (ATCC 33090), *Listeria ivanovii* (ATCC 19119), *Listeria grayi* (ATCC 19120), *Listeria seeligeri* (ATCC 35967), *Acinetobacter lwoffii* (ATCC 15309), *Acinetobacter baumannii* (ATCC 19606), *Acinetobacter calcoaceticus* (ATCC 31299), *Salmonella typhimurium* (ATCC 14028), and *Salmonella choleraesuis* (ATCC 7308).

Antibacterial activity was determined in terms of MIC using the microdilution assay in sterilized 96-well plates in a final volume of 200 μl as follows: bacteria were grown overnight in Luria-Bertani (LB) growth medium [10 g/liter trypton, 5 g/liter yeast extract, and 5 g/liter NaCl (pH 7.4)] and diluted 10,000-fold in growth medium. Stock solutions of the peptides were diluted 10-fold in growth medium. A 100 μl sample of LB-containing bacteria (2–4 × $10^5$ cfu/ml) was added to 100 μl of culture medium containing the test compound (0 to 100 μM in serial 2-fold dilutions). Inhibition of proliferation was determined by optical density measurements (620 nm) after incubation overnight at 37°C.

To assess bactericidal kinetics, bacterial suspensions were added to culture medium containing zero or various peptide concentrations. Bacteria were sampled at various time intervals, subjected to serial 10-fold dilutions, and plated onto LB-agar. Cell counts were determined using the drop plate method (Hoben and Somasegaran, 1982) modified as described previously (Rydlo et al., 2006). Plates were incubated overnight at 37°C and colonies were counted. Statistical data for each experiment were obtained from at least two independent assays performed in triplicate.

### Cytoplasmic Membrane Permeation Assays

The cytoplasmic membrane permeability assay is based on ATP reaction with the enzymatic system luciferin-luciferase, which generates light detectable by a luminometer. The light produced (expressed in relative light units) is proportional to ATP concentration and to the number of viable bacteria originally present in the sample (Gracia et al., 1999). ATP was directly measured in bacterial medium supernatant (suspension of 5 × $10^6$ bacteria with or without OAK or control peptide S4(1–16) at various concentrations). The assay was performed using the kit Cell Titer-Glow Luminescent microbial cell viability assay [Promega; USA 22 (G7570)] according to the producer recommendations. Statistical data for each experiment were obtained from at least two independent assays performed in triplicate.

To verify results obtained with the ATP reaction, β-galactosidase activity was measured in *E. coli* ML35 using *O*-nitrophenyl-β-d-galactopyranoside (ONPG), a nonmembrane-permeative chromogenic substrate, essentially as described previously (Rotem et al., 2008). Briefly, mid-logarithmic phase *E. coli* cells (optical density at 600 nm, 0.05) were washed in PBS (pH 7.4) and incubated with ONPG (1.5 mM) and OAK at 3 or 6 times the MIC value or the positive control dermaseptin S4(1–16) at 25 μM for different time intervals. At the designated time points, sodium carbonate (0.2 M) was added to stop the reaction and enhance light absorbance. The hydrolysis of ONPG to

*O*-nitrophenol was monitored spectrophotometrically at 420 nm. Reported results are from three independent experiments.

### Cytoplasmic Membrane Depolarization

The assay was performed with the fluorescent dye $diSC_3$-5, using *E. coli* ATCC 35218 or *S. aureus* ATCC 29213 as described (Zhang et al., 2000), though the latter bacteria were assayed without incubation in the presence of EDTA.

### Isothermal Titration Calorimetry

Isothermal titrations were performed in a VP-ITC instrument (MicroCal, Inc.) at 30°C, to be above the gel-to-liquid crystalline phase transition of LPS. The OAK was placed in the syringe at a concentration of 200 μM and 10 μl injections into the cell compartment were made. LPS from *E. coli* O111:B4 or LTA from *S. aureus* were place in the cell compartment (volume, 1.4276 ml) at a concentration of 125 μg/ml. All solutions were degassed prior to loading into the calorimeter. The buffer was 10 mM HEPES and 140 mM NaCl (pH 7.4) and was always matched between the syringe and the cell compartment. The heat of dilution of OAK into buffer was subtracted from all the other curves. Data was analyzed with the program Origin 7.0. Quantitative thermodynamic analysis could not be carried out because of the heterogeneity of the LTA and LPS preparations.

### Surface Plasmon Resonance

Binding properties to phospholipid membranes were determined using the BIAcore 2000 optical biosensor system (Biacore Life Science) using small unilamellar vesicles composed of egg yolk phosphatidylcholine (Sigma-Aldrich) and cholesterol (PC:cholesterol, 90:10 molar ratio), 1-palmitoyl-2-oleoyl-*sn*-glycero-3-phosphoethanolamine and 1-palmitoyl-2-oleoyl-*sn*-glycero-3-phosphoglycerol (PE:POPG, 80:20 molar ratio), and 1-palmitoyl-2-oleoyl-*sn*-glycero-3- phosphoglycerol/bovine heart cardiolipin (POPG:CL, 60:40 molar ratio) prepared as described previously (Shalev et al., 2006). Experimental procedures for surface plasmon resonance, analysis of binding kinetics, and calculation of the resulting affinity constants were performed as described previously (Gaidukov et al., 2003).

### DNA Binding Assay

The assay was performed essentially as described previously (Rotem et al., 2008) using pUC19 plasmid from *E. coli* K-12. Briefly, pUC19 plasmid was extracted from bacteria and incubated with OAK for 1 hr, followed by 1 hr incubation with restriction enzymes and run in gel electrophoresis.

### In Vivo Studies

The in vivo efficacy of $C_{12}K\text{-}3\beta_{10}$ was evaluated against *S. aureus* using the thigh infection model. Male ICR mice (20–22 g) were inoculated intramuscularly (using $10^6$ cfu of *S. aureus* ATCC 29213) and treated subcutaneously 2 hr after inoculation. Treatment was evaluated 24 hr after infection: mice were sacrificed and the infected thigh muscles were dissected, homogenized, and plated for cfu enumeration. Procedures, care, and handling of animals were approved by the Technion Animal Care and Use committee.

## ACKNOWLEDGMENTS

This research was supported by the Israel Science Foundation (grant 283/08) and by grant MOP 86608 from the Canadian Institutes of Health Research.

Received: August 26, 2009
Revised: October 7, 2009
Accepted: November 2, 2009
Published: December 23, 2009

## REFERENCES

Boman, H.G., Agerberth, B., and Boman, A. (1993). Mechanisms of action on Escherichia coli of cecropin P1 and PR-39, two antibacterial peptides from pig intestine. Infect. Immun. *61*, 2978–2984.

Bradshaw, J. (2003). Cationic antimicrobial peptides: issues for potential clinical use. BioDrugs *17*, 233–240.

Brogden, K.A. (2005). Antimicrobial peptides: pore formers or metabolic inhibitors in bacteria? Nat. Rev. Microbiol. *3*, 238–250.

Cassell, G.H. (1997). Emergent antibiotic resistance: health risks and economic impact. FEMS Immunol. Med. Microbiol. *18*, 271–274.

Choi, S., Isaacs, A., Clements, D., Liu, D., Kim, H., Scott, R.W., Winkler, J.D., and DeGrado, W.F. (2009). De novo design and in vivo activity of conformationally restrained antimicrobial arylamide foldamers. Proc. Natl. Acad. Sci. USA *106*, 6968–6973.

Couto, M.A., Harwig, S.S., and Lehrer, R.I. (1993). Selective inhibition of microbial serine proteases by eNAP-2, an antimicrobial peptide from equine neutrophils. Infect. Immun. *61*, 2991–2994.

Cudic, M., and Otvos, L., Jr. (2002). Intracellular targets of antibacterial peptides. Curr. Drug Targets *3*, 101–106.

Epand, R.F., Mowery, B.P., Lee, S.E., Stahl, S.S., Lehrer, R.I., Gellman, S.H., and Epand, R.M. (2008a). Dual mechanism of bacterial lethality for a cationic sequence-random copolymer that mimics host-defense antimicrobial peptides. J. Mol. Biol. *379*, 38–50.

Epand, R.M., Rotem, S., Mor, A., Berno, B., and Epand, R.F. (2008b). Bacterial membranes as predictors of antimicrobial potency. J. Am. Chem. Soc. *130*, 14346–14352.

Epand, R.F., Sarig, H., Mor, A., and Epand, R.M. (2009). Cell-wall interactions and the selective bacteriostatic activity of a miniature oligo-acyl-lysyl. Biophys. J. *97*, 2250–2257.

Falla, T.J., Karunaratne, D.N., and Hancock, R.E. (1996). Mode of action of the antimicrobial peptide indolicidin. J. Biol. Chem. *271*, 19298–19303.

Fields, G.B., and Noble, R.L. (1990). Solid phase peptide synthesis utilizing 9-fluorenylmethoxycarbonyl amino acids. Int. J. Pept. Protein Res. *35*, 161–214.

Gaidukov, L., Fish, A., and Mor, A. (2003). Analysis of membrane-binding properties of dermaseptin analogues: relationships between binding and cytotoxicity. Biochemistry *42*, 12866–12874.

Ge, Y., MacDonald, D.L., Holroyd, K.J., Thornsberry, C., Wexler, H., and Zasloff, M. (1999). In vitro antibacterial properties of pexiganan, an analog of magainin. Antimicrob. Agents Chemother. *43*, 782–788.

Giangaspero, A., Sandri, L., and Tossi, A. (2001). Amphipathic alpha helical antimicrobial peptides. Eur. J. Biochem. *268*, 5589–5600.

Gordon, Y.J., Romanowski, E.G., and McDermott, A.M. (2005). A review of antimicrobial peptides and their therapeutic potential as anti-infective drugs. Curr. Eye Res. *30*, 505–515.

Gracia, E., Fernandez, A., Conchello, P., Alabart, J.L., Perez, M., and Amorena, B. (1999). In vitro development of Staphylococcus aureus biofilms using slime-producing variants and ATP-bioluminescence for automated bacterial quantification. Luminescence *14*, 23–31.

Hancock, R.E. (1997). Peptide antibiotics. Lancet *349*, 418–422.

Hancock, R.E., and Sahl, H.G. (2006). Antimicrobial and host-defense peptides as new anti-infective therapeutic strategies. Nat. Biotechnol. *24*, 1551–1557.

Harder, J., Bartels, J., Christophers, E., and Schroder, J.M. (2001). Isolation and characterization of human beta-defensin-3, a novel human inducible peptide antibiotic. J. Biol. Chem. *276*, 5707–5713.

Held-Kuznetsov, V., Rotem, S., Assaraf, Y.G., and Mor, A. (2009). Host-defense peptide mimicry for novel antitumor agents. FASEB J.

Heller, W.T., Waring, A.J., Lehrer, R.I., and Huang, H.W. (1998). Multiple states of beta-sheet peptide protegrin in lipid bilayers. Biochemistry *37*, 17331–17338.

Hoben, H.J., and Somasegaran, P. (1982). Comparison of the pour, spread, and drop plate methods for enumeration of Rhizobium spp. in inoculants made from presterilized peat. Appl. Environ. Microbiol. *44*, 1246–1247.

Howe, J., Andra, J., Conde, R., Iriarte, M., Garidel, P., Koch, M.H., Gutsmann, T., Moriyon, I., and Brandenburg, K. (2007). Thermodynamic analysis of the lipopolysaccharide-dependent resistance of gram-negative bacteria against polymyxin B. Biophys. J. *92*, 2796–2805.

Kirshenbaum, K., Barron, A.E., Goldsmith, R.A., Armand, P., Bradley, E.K., Truong, K.T., Dill, K.A., Cohen, F.E., and Zuckermann, R.N. (1998). Sequence-specific polypeptoids: a diverse family of heteropolymers with stable secondary structure. Proc. Natl. Acad. Sci. USA *95*, 4303–4308.

Liu, D., and DeGrado, W.F. (2001). De novo design, synthesis, and characterization of antimicrobial beta-peptides. J. Am. Chem. Soc. *123*, 7553–7559.

Lohner, K., and Prenner, E.J. (1999). Differential scanning calorimetry and X-ray diffraction studies of the specificity of the interaction of antimicrobial peptides with membrane-mimetic systems. Biochim. Biophys. Acta *1462*, 141–156.

Majerle, A., Kidric, J., and Jerala, R. (2003). Enhancement of antibacterial and lipopolysaccharide binding activities of a human lactoferrin peptide fragment by the addition of acyl chain. J. Antimicrob. Chemother. *51*, 1159–1165.

Mangoni, M.L., Epand, R.F., Rosenfeld, Y., Peleg, A., Barra, D., Epand, R.M., and Shai, Y. (2008). Lipopolysaccharide, a key molecule involved in the synergism between temporins in inhibiting bacterial growth and in endotoxin neutralization. J. Biol. Chem. *283*, 22907–22917.

Pag, U., Oedenkoven, M., Papo, N., Oren, Z., Shai, Y., and Sahl, H.G. (2004). In vitro activity and mode of action of diastereomeric antimicrobial peptides against bacterial clinical isolates. J. Antimicrob. Chemother. *53*, 230–239.

Parisien, A., Allain, B., Zhang, J., Mandeville, R., and Lan, C.Q. (2008). Novel alternatives to antibiotics: bacteriophages, bacterial cell wall hydrolases, and antimicrobial peptides. J. Appl. Microbiol. *104*, 1–13.

Patch, J.A., and Barron, A.E. (2003). Helical peptoid mimics of magainin-2 amide. J. Am. Chem. Soc. *125*, 12092–12093.

Patrzykat, A., Friedrich, C.L., Zhang, L., Mendoza, V., and Hancock, R.E. (2002). Sublethal concentrations of pleurocidin-derived antimicrobial peptides inhibit macromolecular synthesis in Escherichia coli. Antimicrob. Agents Chemother. *46*, 605–614.

Piers, K.L., Brown, M.H., and Hancock, R.E. (1994). Improvement of outer membrane-permeabilizing and lipopolysaccharide-binding activities of an antimicrobial cationic peptide by C-terminal modification. Antimicrob. Agents Chemother. *38*, 2311–2316.

Porter, E.A., Weisblum, B., and Gellman, S.H. (2005). Use of parallel synthesis to probe structure-activity relationships among 12-helical beta-peptides: evidence of a limit on antimicrobial activity. J. Am. Chem. Soc. *127*, 11516–11529.

Radzishevsky, I.S., Rotem, S., Zaknoon, F., Gaidukov, L., Dagan, A., and Mor, A. (2005). Effects of acyl versus aminoacyl conjugation on the properties of antimicrobial peptides. Antimicrob. Agents Chemother. *49*, 2412–2420.

Radzishevsky, I., Krugliak, M., Ginsburg, H., and Mor, A. (2007a). Antiplasmodial activity of lauryl-lysine oligomers. Antimicrob. Agents Chemother. *51*, 1753–1759.

Radzishevsky, I.S., Rotem, S., Bourdetsky, D., Navon-Venezia, S., Carmeli, Y., and Mor, A. (2007b). Improved antimicrobial peptides based on acyl-lysine oligomers. Nat. Biotechnol. *25*, 657–659.

Radzishevsky, I.S., Kovachi, T., Porat, Y., Ziserman, L., Zaknoon, F., Danino, D., and Mor, A. (2008). Structure-activity relationships of antibacterial acyl-lysine oligomers. Chem. Biol. *15*, 354–362.

Rotem, S., and Mor, A. (2009). Antimicrobial peptide mimics for improved therapeutic properties. Biochim. Biophys. Acta *1788*, 1582–1592.

Rotem, S., Radzishevsky, I.S., Bourdetsky, D., Navon-Venezia, S., Carmeli, Y., and Mor, A. (2008). Analogous oligo-acyl-lysines with distinct antibacterial mechanisms. FASEB J. *22*, 2652–2661.

Rydlo, T., Rotem, S., and Mor, A. (2006). Antibacterial properties of dermaseptin S4 derivatives under extreme incubation conditions. Antimicrob. Agents Chemother. *50*, 490–497.

Sahl, H.G., Pag, U., Bonness, S., Wagner, S., Antcheva, N., and Tossi, A. (2005). Mammalian defensins: structures and mechanism of antibiotic activity. J. Leukoc. Biol. *77*, 466–475.

Sarig, H., Rotem, S., Ziserman, L., Danino, D., and Mor, A. (2008). Impact of self-assembly properties on antibacterial activity of short acyl-lysine oligomers. Antimicrob. Agents Chemother. *52*, 4308–4314.

Shai, Y. (2002). Mode of action of membrane active antimicrobial peptides. Biopolymers *66*, 236–248.

Shalev, D.E., Rotem, S., Fish, A., and Mor, A. (2006). Consequences of N-acylation on structure and membrane binding properties of dermaseptin derivative K4-S4-(1-13). J. Biol. Chem. *281*, 9432–9438.

Tanford, C. (1980). The Hydrophobic Effect: Formation of Micelles and Biological Membranes (New York: John Wiley & Sons).

Tew, G.N., Liu, D., Chen, B., Doerksen, R.J., Kaplan, J., Carroll, P.J., Klein, M.L., and DeGrado, W.F. (2002). De novo design of biomimetic antimicrobial polymers. Proc. Natl. Acad. Sci. USA *99*, 5110–5114.

Wu, M., Maier, E., Benz, R., and Hancock, R.E. (1999). Mechanism of interaction of different classes of cationic antimicrobial peptides with planar bilayers and with the cytoplasmic membrane of Escherichia coli. Biochemistry *38*, 7235–7242.

Zaknoon, F., Sarig, H., Rotem, S., Livne, L., Ivankin, A., Gidalevitz, D., and Mor, A. (2009). Antibacterial properties and mode of action of a short acyl-lysyl oligomer. Antimicrob. Agents Chemother. *53*, 3422–3429.

Zasloff, M. (2002). Antimicrobial peptides of multicellular organisms. Nature *415*, 389–395.

Zetola, N., Francis, J.S., Nuermberger, E.L., and Bishai, W.R. (2005). Community-acquired meticillin-resistant Staphylococcus aureus: an emerging threat. Lancet Infect. Dis. *5*, 275–286.

Zhang, L., Dhillon, P., Yan, H., Farmer, S., and Hancock, R.E. (2000). Interactions of bacterial cationic peptide antibiotics with outer and cytoplasmic membranes of Pseudomonas aeruginosa. Antimicrob. Agents Chemother. *44*, 3317–3321.

 